STUDY ON PHASE RELATION AND SYNTHESIS OF PYROCHLORE IN THE SYSTEM OF Ca-Ce-Zr-O

S. C. Chae, Y. N. Jang, I. K. Bae
Korea Institute of Geoscience and Mineral Resources
30 Gajeong-dong, Yuseong-gu, Daejeon, 305-350, Korea

S.V. Yudintsev
Institute of Geology of Ore Deposits, Petrography, Mineralogy and Geochemistry, Staromonetny 35, Moscow 119017, Russia

ABSTRACT

Pyrochlore was known as one of the most promising materials for the immobilization of actinide-rich high level waste. We have carried on the synthesis of pyrochlore ($CaCeZr_xTi_{2-x}O_7$, x=0.2-2.0) and examination of the phase relation in the system of Ca-Ce-Zr-Ti-O. Using the Cold pressing and sintering (CPS) method, the mixture of $CaCO_3$, CeO_2, ZrO_2 and TiO_2 oxides was pressed, and sintered at 1200-1600^oC for 20 hr. The optimum synthetic temperatures of oxides with pyrochlore or fluorite-type structures at various stoichiometric compositions ranged from 1400 to 1600^oC. Even at the optimum conditions, major pyrochlore or fluorite-type oxides coexisted with minor perovskite, CeO_2 or $Ce_{0.75}Zr_{0.25}O_2$ (CeZrO). It was confirmed that pyrochlore and fluorite structures were stable in the range of x=0.2-0.6 and x=1.0-2.0, respectively. In accordance with SEM/EDS data, pyrochlore or fluorite-type oxides have non-stoichiometric compositions with deficient Ca and Ti and excessive Zr and Ce as x value increased. We inferred that non-stoichiometric compositions of the phases are explained by coexistence of perovskite, CeO_2 or CeZrO phase along with pyrochlore or fluorite-type oxides even at optimum synthetic temperatures.

INTRODUCTION

Liquid high level waste sludges originated from the reprocessing of the spent nuclear fuel contained very dangerous radionuclides, in the first turn long-lived actinides. Therefore, immobilizing matrices, which can fix them, were required. The early history of the development of nuclear waste forms is summarized by Lutze [1]. These efforts, mainly in the 1950s, focused on the incorporation of radioactive waste into glasses of widely varying compositions. The first radioactive wastes were incorporated into a nepheline syenite (a silica-deficient igneous rock)

glass at Chalk River, Canada [2]. However, glass is thermodynamically unstable and subjected to devitrification. As a result of this, its chemical durability decreases, and the possibility exists that radionuclides can be released to the environment [3].

In the mid to late 1970s, considerable interest in alternative nuclear waste forms to glass began with the development of supercalcine by McCarthy [4] and tailored ceramics by Harker [5] at the Rockwell International Science Center in the United States. Ringwood [6] and his colleagues [7] at the Australian National University closely followed this work with the initial development phase of Synroc. Ringwood's concept for Synroc called for a material based on minerals that were known, from the geological record, to be highly durable and capable of incorporating the actinides, Sr, Cs, and other fission products present in reprocessed spent fuel. Ewing [8], Ewing and Haaker [9] and Haaker and Ewing [10] at the University of New Mexico also began to formulate ideas on the application of metamict minerals to the study of ceramic nuclear waste forms. The development of Synroc and other ceramic nuclear waste forms sparked a 10-yr burst of mineralogical investigations of pyrochlore group minerals, zircon, zirconolite, and other radioactive minerals during the 1980's, primarily involving Ewing's group and co-investigators from Sandia National Laboratories, Los Alamos National Laboratory, and the Boeing Company [11].

The study to develop the nuclear waste form has continued through the 1990's to present [12-20]. Among these materials, pyrochlore is one of a number of candidate materials proposed for the immobilization of actinide-rich wastes, and has recently been selected as a key component in the synroc-based pyrochlore-rich ceramics for the geological immobilization of excess weapons Pu [17].

The pyrochlores typically exhibit $[A_2]^{VIII}[B_2]^{VI}O_7$ stoichiometry, where actinides and lanthanides are incorporated on the A-site, and either Ti, Hf, Sn or Zr occupies the B-site. It has a fluorite-derived structure (space group: Fd3m) where one eighth of oxygens are missing. Two different structural sites for cations (A- and B-sites) exist, resulting in the cell parameter of pyrochlore, which is twice that of the fluorite lattice.

The synthetic studies in various systems are required, because the physicochemical properties of pyrochlore vary with the chemical composition. For examples, $Gd_2Ti_2O_7$ and $Gd_2Zr_2O_7$ have similar composition, but $Gd_2Ti_2O_7$ can be synthesized at relatively lower temperature (1300^oC), whereas $Gd_2Zr_2O_7$ is synthesized at a temperature of higher than 300^oC than that of $Gd_2Ti_2O_7$. Also, it was known that $Gd_2Zr_2O_7$ containing 10 weight percent Pu-239 will be radiation

resistant for at least 30 million years, whereas $Gd_2Ti_2O_7$ will completely amorphise in less than 800 years under repository conditions [21-22].

It is important to study not only the synthesis and characterization of pyrochlore but also the phase relation in various systems. Especially, the study on the phase relation will be applied to fundamental data for developing new promising matrices.

In this study, we intend to propose the formation, phase relation, and optimum condition for pyrochlore fabrication in the system of Ca-Ce-Zr-Ti-O using Ce, which is similar to valance and ionic radii of Pu, as an imitator of Pu.

Experimental

The synthesis of pyrochlore was performed by CPS method. $CaCO_3$ (High Purity Chemicals, 4N), TiO_2 (Rare Metallic Co., Ltd., 3N) CeO_2 (Johnson Mattey, 3N), and ZrO_2 (Rare Metallic Co., 3N) were used as starting materials. These powders mixed in the appropriate ratios, ($CaCeZr_xTi_{2-x}O_7$: x = 0.2, 0.6, 1.0, 1.4, 1.8) with alcohol, using an alumina mortar and pestle. The mixed powders were pressed into pellets (10-mm diameter x 2-mm height) at a pressure of 400 kg/cm^2. The pellets were sintered at 1200-1600^{o}C for 20 hr in the oxygen atmosphere for stabilization of Ce in tetravalent state. Phase identification was determined by X-ray diffraction (reflection mode, CuKa radiation) using a Phillips X'pert MPD X-ray diffractometer attached with a graphite monochrometer. The compositions of synthetic phases were analyzed with a SEM/EDS analyzer.

XRD results

$CaCeZr_xTi_{2-x}O_7$ in case of x=0.2: At 1200^{o}C, CeO_2 revealed the strongest diffraction intensity, and perovskite and pyrochlore coexisted with minor TiO_2. The diffraction intensity of pyrochlore increased with increasing temperature. Instead, those of perovskite and CeO_2 gradually decreased. At 1300^{o}C, TiO_2, which is one of starting materials, disappeared and pyrochlore first showed the strongest diffraction intensity. The sample completely melted at 1600^{o}C, a maximum sintering temperature in this batch composition. The diffraction intensity of pyrochlore and coexisting phases did not change between 1300^{o}C and 1500^{o}C. It allows one to conclude that the system attained the equilibrium state (Fig. 1a and Table I).

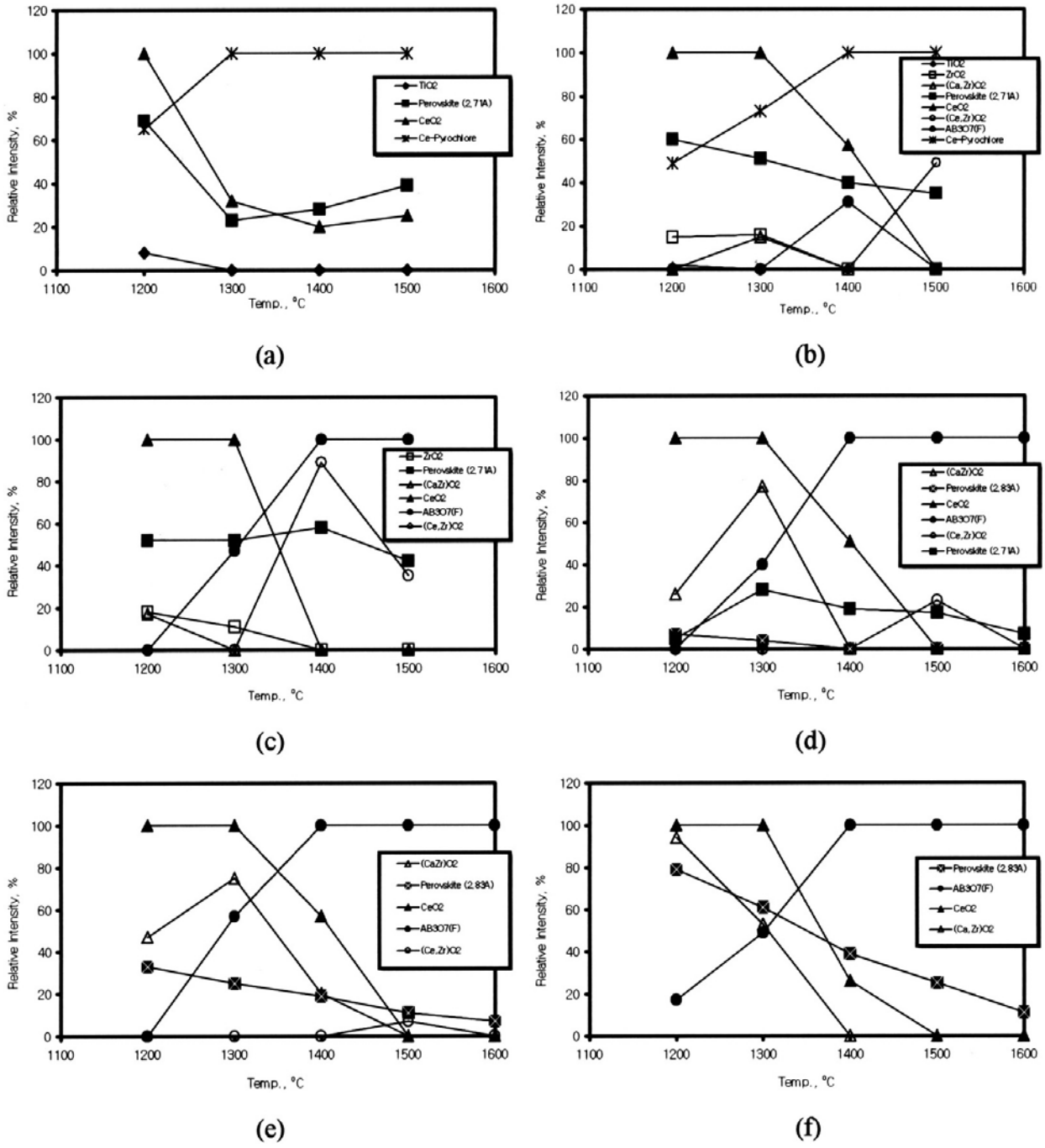

Fig. 1. Relative intensities of phases in the matrices synthesized from $CaCeZr_xTi_{2-x}O_7$. (a) x=0.2, (b) x=0.6, (c) x=1.0, (d) x=1.4, (e) x=1.8 and (f) x=2.0.

Table I. Relative Intensities of Phases Formed from Various Composition Systems. Results for the $CaCeTi_2O_7$ nominal composition (x=0) are taken from Laverov et al., 2003.

Temp.	hrs	TiO_2 (3.25A)	ZrO_2 (3.16A)	CaZrO (2.97A)	Pero. (2.71A)	Pero (2.83A)	CeO_2 (3.12A)	CeZrO (3.09A)	A_3BO_7 (Flu) (3.01A)	Pyro (2.93A)
X=0.0										
1250	50	6	-	-	28	-	19	-	-	100
1270	40	<5	-	-	19	-	25	-	-	100
1300	5	<5	-	-	25	-	34	-	-	100
1300	10	<5	-	-	26	-	26	-	-	100
1300	20	-	-	-	13	-	12	-	-	100
1350	40	-	-	-	17	-	13	-	-	100
1400	1	<5	-	-	33	-	23	-	-	100
1400	3	-	-	-	32	-	22	-	-	100
1400	5	-	-	-	29	-	23	-	-	100
X=0.2										
1200	20	8	-	-	69	-	100	-	-	65
1300	20	-	-	-	23	-	32	-	-	100
1400	20	-	-	-	28	-	20	-	-	100
1500	20	-	-	-	39	-	25	-	-	100
1600	20	melt								
X=0.6`										
1200	20	2	15	-	60	-	100	-	-	49
1300	20	-	16	15	51	-	100	-	-	73
1400	20	-	-	-	40	-	57	-	31	100
1500	20	-	-	-	35	-	-	49	-	100
1600	20	melt								
X=1.0										
1200	20	-	18	17	52	-	100	-	-	-
1300	20	-	11	-	52	-	100	-	47	-
1400	20	-	-	-	58	-	-	89	100	-
1500	20	-	-	-	42	-	-	35	100	-
1600	20	melt								
X=1.4										
1200	20	-	-	26	5	7	100	-	-	-
1300	20	-	-	77	28	4	100	-	40	-
1400	20	-	-	-	19	-	51	-	100	-
1500	20	-	-	-	17	-	-	23	100	-
1600	20	-	-	-	7	-	-	-	100	-
X=1.8										
1200	20	-	-	47	-	33	100	-	-	-
1300	20	-	-	75	-	25	100	-	57	-
1400	20	-	-	20	-	19	57	-	100	-
1500	20	-	-	-	-	11	-	7	100	-
1600	20	-	-	-	-	7	-	-	100	-
X=2.0										
1200	20	-	-	94	-	79	100	-	17	-
1300	20	-	-	53	-	61	100	-	49	-
1400	20	-	-	-	-	39	26	-	100	-
1500	20	-	-	-	-	25	-	-	100	-
1600	20	-	-	-	-	11	-	-	100	-

Abbreviations: CaZrO-$Ca_{0.15}Zr_{0.85}O_{1.85}$; Pero (2.71A)-perovskite(2.71A); Pero (2.83A)-perovskite(2.83A); CeZrO-$Ce_{0.75}Zr_{0.25}O_2$; A_3BO_7 (Flu)-fluorite structure oxides; Pyro-pyrochlore

$CaCeZr_xTi_{2-x}O_7$ in case of x=0.6: At 1200°C, CeO_2 displayed the strongest diffraction intensity and coexisted with TiO_2, baddeleyite (monoclinic-form of ZrO_2), pyrochlore and perovskite (Fig. 1b and Table I). At 1300°C, CeO_2 was observed as a main phase, the disappearance of TiO_2, the formation of Ca-Zr-O oxide ($Ca_{0.15}Zr_{0.85}O_{1.85}$: CaZrO) and the increase of pyrochlore were detected. Pyrochlore first showed the strongest intensity at 1400°C, whilst amounts of perovskite and CeO_2 decrease gradually.

The characteristics features of this composition are the temporary formation and disappearance of CaZrO, and appearance of fluorite structured oxide (A_3BO_7: fluorite) and Ce-Zr-O oxide ($Ce_{0.75}Zr_{0.25}O_2$: CeZrO) as intermediate phases. The specimen melted at 1600°C as like as one with composition at x=0.2.

$CaCeZr_xTi_{2-x}O_7$ in case of x=1.0: Baddelyite, CeO_2, perovskite and CaZrO were observed at 1200°C (Fig. 1c and Table I). At 1300°C, fluorite-type oxide was found, and CaZrO appeared, but the intensities of baddelyite, perovskite and CeO_2 were similar to those at 1200°C. At 1400°C and 1500°C, fluorite-type oxide showed the strongest intensity, and CeZrO was formed simultaneously with disappearance of CeO_2 and baddelyite. The specimen melted at 1600°C just like the batches in the compositional range with x = 0.2-0.6.

The characteristics of this composition are the formation of the fluorite-type oxide instead of pyrochlore structure phase. It indicates that the structure transition attributes to the content of zirconium in the precursor.

$CaCeZr_xTi_{2-x}O_7$ in case of x=1.4: At 1200°C, CeO_2 showed the strongest intensity and two kinds of perovskites (d=2.71A and d=2.83A, d: d-spacing value at strongest diffraction intensity in each phase) coexisted with CaZrO (Fig. 1d and Table I). At 1300°C, fluorite-type oxide was also observed, CeO_2 showed the strongest diffraction intensity, and the intensities of CaZrO and 2.71A-perovskite (perovskite-I) increased, whereas amount of 2.83A-perovksite (perovskite-II) decreased. At 1400°C, fluorite-structure oxide showed the strongest diffraction intensity, and the decrease of CeO_2 and perovskite-I and the disappearance of perovskite-II and CaZrO were observed. With the increase of temperature, disappearance of CeO_2, and the temporary existence of CeZrO were observed. As a result, perovskite-I and oxide with fluorite lattice were final products at 1600°C, which was maximum sintering temperature in this experiment.

One of features of this composition was the existence of perovskite-I and perovskite-II. It suggested that perovskite-I would transform into perovskite-II with the increase of the content of

Zr, because perovskite-I was observed as a main phase between them at x=0.2-1.0.

$CaCeZr_xTi_{2-x}O_7$ in case of x=1.8 and x=2.0: The phase relation at x=1.8 was similar to that at x =2.0. Accordingly, we intend to describe only about the result for initial batch composition with x=1.8. At 1200^{o}C, CeO_2 showed the strongest diffraction intensity, and coexisted with CaZrO and perovskite-II (Fig. 1e and Table I). At 1300^{o}C, fluorite first formed, and the decrease of perovskite-II and the increase of CaZrO were observed. With the increase of temperature, CaZrO, perovskite-II and CeO_2 decrease, whereas fluorite showed the strongest diffraction intensity. Although CeZrO, a temporary phase, was observed at 1500^{o}C, fluorite coexisted with minor perovskite-II at 1600^{o}C, which was the maximum sintering temperature in this experiment.

The feature of this composition was the absence of perovskite-I, which was observed at x=0.2-1.4. As mentioned above, it supported the fact that perovskite-II was stable phase only for the batch compositions containing high zirconium content.

SEM/EDS Analysis

To observe the change of chemical compositions of the phases fabricated from different batch compositions, SEM/EDS analysis was carried out. In sample sintered at x=0.2 (Fig. 2a), pyrochlore composed a basis of matrix, and CeO_2 and minor perovskite were observed as phenocrysts (Fig. 3a). Sample sintered at x=0.6 (Fig. 2b) was almost similar to one at x=0.2, the only difference between them is the existence of CeZrO instead of CeO_2 (Fig. 3b). CeZrO phase was produced from the reaction of CeO_2 and ZrO_2. Sample sintered at x=1.0 consisted of phases as same as at x=0.6, but showed the smaller grain size by insufficient reaction time (Fig. 3c). At x=1.4 to x=1.8, pyrochlore and perovskite coexisted and their grain sizes were 30-50□. These relative large grain size of phases was obviously due to the higher sintering temperature (1600 ^{o}C) compared with the other samples (Fig. 3d and Fig. 3e). The compositions of pyrochlores were close to initial stoichiometric compositions (Table II). However, those of fluorite-type oxides showed considerable difference compared with stoichiometric compositions of initial batch in that Ca was deficient (Ca=0.3-0.5 atoms per formula unit, apfu) and Ce was slightly excessive (Ce=0.9-1.3 apfu), so their sum (Ca+Ce=1.4-1.8 apfu) were also deficient. Such phenomena were observed in elements occupying the six-coordinated site too. Namely, the contents of Zr were in excess, whereas those of Ti were deficient. We inferred that such non-stoichiometric compositions of pyrochlore and fluorite-structure oxides resulted from the existence of CeZrO, CeO_2 or perovskite at all synthetic conditions.

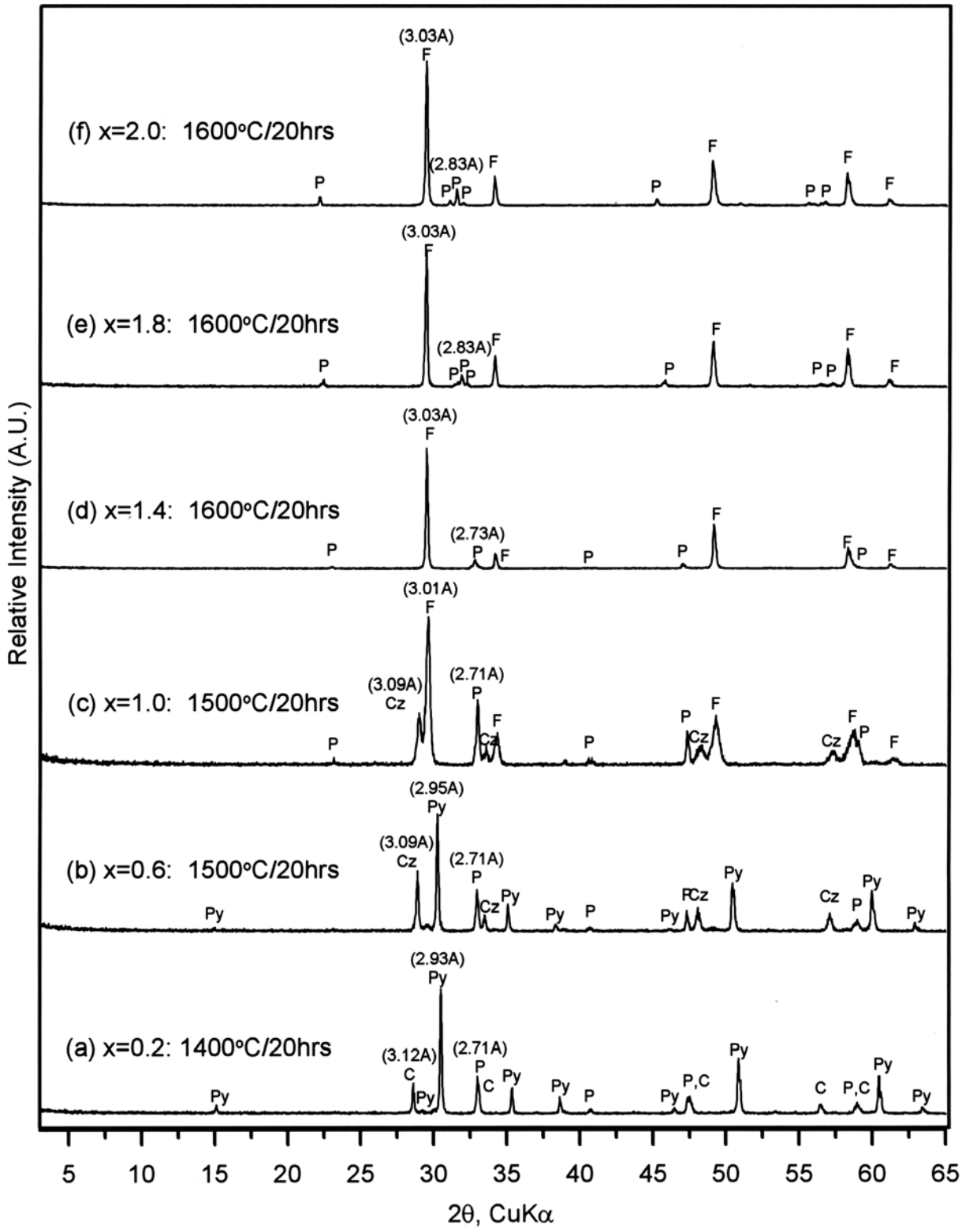

Fig. 2. XRD patterns of phases synthesized in optimum conditions from $CaCeZr_xTi_{2-x}O_7$ batch composition. Abbreviation: Py (Pyrochlore), P (Perovskite), C (CeO_2; Cerianite), Cz (CeZrO), F (Fluorite)

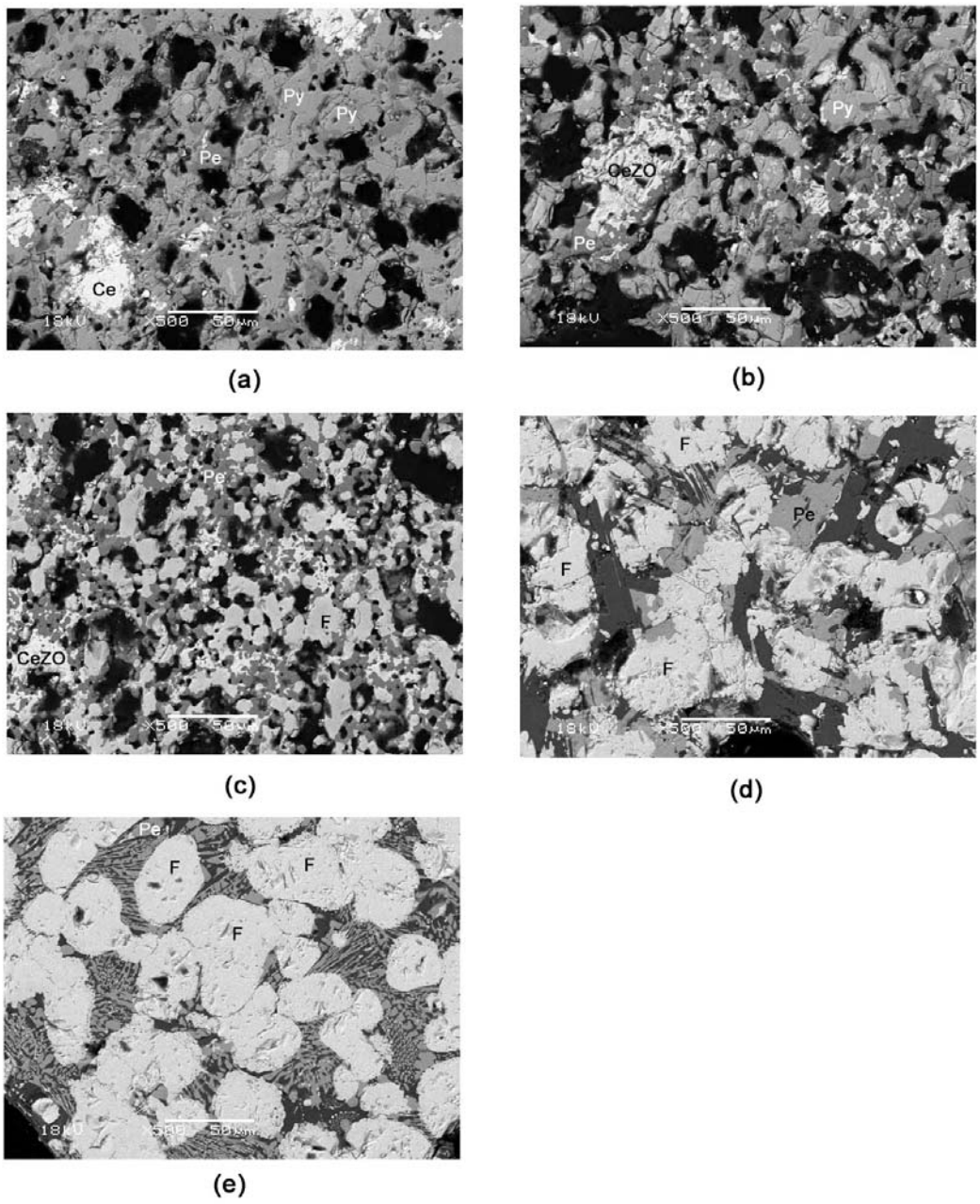

Fig. 3. Back scattered electron images of specimens synthesized from batch compositions, $CaCeZr_xTi_{2-x}O_7$ (a) at x=0.2, (b) at x=0.6, (c) at x=1.0, (d) at x=1.4 and (e) at x=1.8. Abbreviation: Py (pyrochlore), F (fluorite), Pe (perovskite), CeZO ($Ce_{0.75}Zr_{0.25}O_2$)

Table II. Chemical Compositions of Pyrochlore, Fluorite and Perovskite Synthesized from Batch Compositions, $CaCeZr_xTi_{2-x}O_7$ (x=0.2-1.8).

Compositions	Temp.	CaO	CeO_2	ZrO_2	TiO_2	Chemical composition	Phases
X=0.2	1400	13.36	39.06	10.83	35.75	$Ca_{0.9}Ce_{0.9}Zr_{0.3}Ti_{1.8}O_7$	Py
		12.95	42.05	5.78	39.21	$Ca_{0.9}Ce_{1.0}Zr_{0.2}Ti_{1.9}O_7$	Py
X=0.6	1500	11.23	36.72	25.24	26.81	$Ca_{0.8}Ce_{0.9}Zr_{0.8}Ti_{1.4}O_7$	Py
		11.47	37.57	25.69	25.27	$Ca_{0.9}Ce_{0.9}Zr_{0.9}Ti_{1.3}O_7$	Py
X=1.0	1500	6.22	34.23	55.28	4.27	$Ca_{0.5}Ce_{0.9}Zr_{2.1}Ti_{0.3}O_7$	F
		5.71	36.25	53.88	4.16	$Ca_{0.5}Ce1.0Zr_{2.0}Ti_{0.2}O_7$	F
		5.92	33.11	55.92	5.05	$Ca_{0.5}Ce_{0.9}Zr_{2.1}Ti_{0.3}O_7$	F
X=1.4	1600	3.32	40.82	54.13	1.73	$Ca_{0.3}Ce_{1.1}Zr_{2.1}Ti_{0.1}O_7$	F
		3.61	40.36	54.95	1.08	$Ca_{0.3}Ce_{1.1}Zr_{2.2}Ti_{0.1}O_7$	F
		3.44	39.16	56.38	1.02	$Ca_{0.3}Ce_{1.1}Zr_{2.2}Ti_{0.1}O_7$	F
X=1.8	1600	3.65	42.13	53.02	1.20	$Ca_{0.3}Ce_{1.2}Zr_{2.1}Ti_{0.1}O_7$	F
		4.49	45.53	48.43	1.55	$Ca_{0.4}Ce_{1.3}Zr_{1.9}Ti_{0.1}O_7$	F
		5.16	45.24	48.37	1.23	$Ca_{0.5}Ce_{1.3}Zr_{1.9}Ti_{0.1}O_7$	F

Py: pyrochlore and F: fluorite-structure oxides

Discussion

Perovskite, pyrochlore, CaZrO, CeZrO and fluorite-type oxides were observed in the system of Ca-Ce-Zr-Ti-O. In some of samples, un-reacted initial oxides were also present. The diffraction intensities of perovskite, CeO_2 and pyrochlore did not changed with the increase of temperature from 1300^{o}C to 1500 ^{o}C at x=0.2. Moreover, the number of coexisted phases, such as CeZrO, CeO_2 or perovskite and their intensities decreased with increase of temperature. These two results indicated that equilibrium state could be easily attained at lower Zr content and higher temperature. However, some Ce could reduce into Ce^{3+} at high temperatures and it also influenced phase relations and compositions in the ceramics along with the non-stoichiometric composition of pyrochlore or fluorite structured oxides as stated above.

Such results of the phase relation and equilibrium state were similar to those of study [23] in the Ca-Ce-Ti-O system (x=0; hypothetical pyrochlore end member: $CaCeTi_2O_7$). Namely, phases formation process was completed through 20 hours at 1250-1300^{o}C, and took only 1 hour at 1400^{o}C in the system of Ca-Ce-Ti-O. Also, three phases - major pyrochlore with minor perovskite and cerianite were observed even at the longest sintering (Table I). It may be

explained by non-stoichiometry of the pyrochlore typical of all phases with general formula $CaA^{4+}Ti_2O_7$, where "A^{4+}" – actinides (U, Th, Pu) or Ce. Deviation of the stoichiometric phases from the ideal formula consists in Ca to "A^{4+}". The atomic ratio ranged from 1.1 to 2.0 which is higher than the value (1.0) in the ideal composition.

The other reason for additional perovskite phase formation is existence of some Ce in trivalent form [20].

The d-spacings of perovskite and pyrochlore (or fluorite at high Zr content) increased with the content of Zr in the composition of precursor (Table I). In $CaCeZr_xTi_{2-x}O_7$ compositions, 2.71A-perovskite (perovskite-I) increased to x=1.4, but 2.83A-perovskite (perovskite-II) was above x=1.4 (Table I). Transformation of pyrochlore into fluorite-type oxide was observed distinctly at high Zr content. Namely, 2.93A-pyrochlore was observed up to x=0.6, but 3.01A-fluorite instead of pyrochlore above x=1.0. This transition has been observed in $Gd_2Zr_2O_7$ pyrochlore too. However, its transition was related with temperature in that pyrochlore structure was stable below 1530^{o}C whereas fluorite structure was stable above 1530^{o}C. In contrast to $Gd_2Zr_2O_7$, the transition in $CaCeZr_xTi_{2-x}O_7$ was depended on composition. Such existence of two closely structured phases was to due to the difference of ionic radii of Zr and Ti occupied the 6-coordinated site and those of Ca and Ce occupied the 8-coordinated site. The stability of $[A_2]^{VIII}[B_2]^{VI}O_7$ pyrochlore is governed by the ionic radii ratio of the [A] and [B] site cations (r_A^{VIII}/r_B^{VI}). The range of pyrochlores stability extends from r_A^{VIII}/r_B^{VI}=1.46 for $Gd_2Zr_2O_7$ to r_A^{VIII}/r_B^{VI}=1.78 for $Sm_2Ti_2O_7$. For smaller ionic radii ratios, r_A^{VIII}/r_B^{VI}<1.46, anion-deficient fluorite is the stable structure, whereas the monoclinic structure is typical of phases for ionic radii ratios r_A^{VIII}/r_B^{VI}>1.78 [16].

Based on the results calculated from each batch composition, all synthetic pyrochlores were expected to have pyrochlore structure with the only exception of $CaCeZr_2O_7$ (r_A^{VIII}/r_B^{VI}=1.45) (Table III). However, pyrochlore was formed only at x≤0.6 and fluorite structure was observed at x>1.0, being independent of the results of the ionic radii ratio calculated from the initial batch compositions. This conclusion could be interpreted from the results of calculated composition from EDS data. Compositions and ionic radii ratios of pyrochlore and fluorite were as follows; $[Ca_{0.9}Ce_{0.9-1.0}][Zr_{0.2-0.3}Ti_{1.8-1.9}]O_7$ (r_A^{VIII}/r_B^{VI}=1.679-1.696) at x=0.2, $[Ca_{0.8-0.9}Ce_{0.9}][Zr_{0.8-0.9}Ti_{1.3-1.4}]O_7$ (r_A^{VIII}/r_B^{VI}=1.603-1.608) at x=0.6, $[Ca_{0.5}Ce_{0.9-1.0}][Zr_{2.0-2.1}Ti_{0.2-0.3}]O_7$ (r_A^{VIII}/r_B^{VI}=1.439-1.449) at x=1.0, $[Ca_{0.3}Ce_{1.1}][Zr_{2.1-2.2}Ti_{0.1}]O_7$ (r_A^{VIII}/r_B^{VI}=1.397-1.398) at x=1.4 and $[Ca_{0.3-0.5}Ce_{1.2-1.3}][Zr_{1.9-2.1}Ti_{0.1}]O_7$ (r_A^{VIII}/r_B^{VI}=1.399-1.410) at x=1.8.

It was in a good agreement with the results of XRD that phases synthesized in the ranges of x=0.2-0.6 and x=1.0-1.8 belonged to the stability ranges of pyrochlore and fluorite structures, respectively.

Table III. Optimum Conditions, Lattice Parameters and Average Radii of Elements with Coordinated Sites in Each System.

Compositions	Optimum Conditions		Average Ionic Radii (unit: angstrom)		A/B
	Temp. ^{o}C	Time, hrs	A	B	
X=0.2	1400	20	1.045	0.617	1.6951
X=0.6	1500	20	1.045	0.640	1.6341
X=1.0	1500	20	1.045	0.663	1.5774
X=1.4	1600	20	1.045	0.686	1.5244
X=1.8	1600	20	1.045	0.709	1.4749
X=2.0	1600	20	1.045	0.720	1.4514

A: average ionic radii of Ca and Ce in 8-coordinated site, B: average ionic radii of Zr and Ti in 6-coordinated site.

CONCLUSIONS

This study included the synthesis of pyrochlore, and research of phase relation in the system of Ca-Ce-Zr-Ti-O. Pyrochlore, fluorite-structure oxides, perovskite, CaZrO and CeZrO phases were synthesized. These systems resulted in the existence of pyrochlore (x=0.2-0.6) or fluorite (x=1.0-2.0) as final phases. Their formation were related to the ionic radii ratio of the elements occupied the 8-coodinated and the 6-coordinated sites. The non-stoichiometric compositions of pyrochlore or fluorite resulted in the appearance of minor perovskite, CeO_2 or CeZrO in all the conditions of experiments (1400^{o}C-1600^{o}C).

REFERENCES

1. W. Lutze, "Silicate glasses," In: Radioactive Waste Forms for the Future, Lutze, W. and Ewing, R.C. (Eds.). 1-159. North-Holland, Amsterdam (1988).
2. R. C. Ewing, W. J. Weber, and F. W. Clinard Jr., Progress in Nuclear Energy, 29, 2, 63-127 (1995).
3. I.A. Sobolev, S.V. Stefanovsky and F.A. Lifanov, "Synthetic melted rock-type wasteforms," MRS Sympo. Proc. 353, 833-840 (1995).
4. G. J. McCarthy, "High-level waste ceramics: materials considerations, process simulation

and product characterization," Nucl. Technol. 32, 92 (1977).

5. A. B. Harker, A. B., In: Lutze, W. and Ewing, R.C. (Eds.), Radioactive Waste Forms for the Future, North-Holland, Amsterdam, 335 (1988).
6. A. E. Ringwood, "Safe Disposal of Hihg Level Nuclear Reactor Wastes": A New Strategy, Australian national University Press, Canberra (1978).
7. A. E. Ringwood, S. E. Kesson, N. G. Ware, W. Hibberson, and A. Major, "Immobilization of high level nuclear reactor wastes in SYNROC," Nature, 278, 5701, 219-223 (1979).
8. R. C. Ewing, "Metamict mineral alteration: An implication for radioactive waste disposal," Science, 192, 1336-1337 (1976).
9. R. C. Ewing, and R. F. Haaker, "The metamict state: Implications for radiation damage in crystalline waste forms," Nuclear and Chemical Waste Management, 1, 51-57 (1980).
10. R. F. Haaker, and R. C. Ewing, "Uranium and thorium minerals: Natural analogues for crystalline radioactive waste forms," In Scientific Basis for Nuclear Waste Management, Vol. 2, C. M. Northrup, Jr., Ed., Plenum Press, New York, 281-288 (1980).
11. G. R. Lumpkin, "Alpha-decay damage and aqueous durability of actinide host phases in natural systems," J. Nucl. Mat., 289, 136-166 (2001).
12. E. R. Vance, B. D. Begg, R. A. Day, and C. J. Ball, "Zirconolite-rich ceramics for actinide wastes," In: Scientific Basis for Nuclear Waste Management-XVIII. MRS Symposia Proceedings, Vol.353, Pt.2, p.767-774 (1995).
13. S. Luo, X. Zhu, and B. Tang, "Actinides containment by using zirconolite-rich Synroc," In: Proceedings of International Meeting on Nuclear and Hazardous Waste Management (Spectrum 98), American Nuclear Society, La Grange Park, IL, p.829-833 (1998).
14. N. K. Kulkarni, S. Sampath, and V. Venugopal, "Preparation and characterization of Pu-pyrochlore: $[La_{1-x}Pu_x]_2Zr_2O_7$ (x=0-1)," J. Nucl. Mater., 281, 248-250 (2000).
15. A. J. Feighery, J. T. S. Irvine, and S. Zheng, S., "Phase relation at 1500 in the ternary system ZrO_2-Gd_2O_3-TiO_2," J. Solid State Chemistry, 160, 302-306 (2001).
16. B. D. Begg, N. J. Hess, D. E. McCready, S. Thevuthasan, and W. J. Weber, "Heavy-ion irradiation effects in $Gd_2(Ti_{2-x}Zr_x)O_7$ pryochlore," J. Nucl. Mat, 289, 188-193 (2001).
17. B. D. Begg, N. J. Hess, W. J. Weber, R. Devanathan, J. P. Icenhower, S. Thevuthasan, and B. P. McGrail, "Heavy-ion irradiation effects on structures and acid dissolution of pyrochlore," J. Nucl. Mat, 228, 208-216 (2001).
18. N. P. Laverov, S. V. Yudintsev, S. V. Stefanovsky, and Y. N. Jang, "New actinide matrix with pyrochlore structure," Doklady of the Russian Academy of Sciences, 381A, 9, 1053-1056 (2001).
19. N. P. Laverov, S. V. Yudintsev, S. V. Stefanovsky, Y. N. Jang, M. I. Lapina, A. V. Sivtsov, and R. C. Ewing, "Phase transformations during synthesis of actinide matrices," Doklady of

the Russian Academy of Sciences, 385A, 6, 671-675 (2002).

20. Yu. A. Teterin, S. V. Stefanovskii, S. V. Yudintsev, G. N. Bek-Uzarov, A. Yu. Tetrerin, K. I. Maslakov, and I. O. Utkin, “X-ray photoelectron study of calcium cerium titanate ceramics,” Russian Journal of Inorganic Chemistry, 49, 1, 87-94 (2004).
21. W. J. Weber, and R. C. Ewing, “Plutonium immobilization and radiation effects,” Science, 289, 2051-2052 (2000).
22. S. X. Wang, B. D. Begg, L. M. Wang, R. C. Ewing, W. J. Weber, and K. V. G. Kutty, “Radiation stability of gadolinium zirconate: A waste form for plutonium disposition,” J. Mater. Res. 14, 12, 4470-4473 (1999).
23. N. P. Laverov, S. V. Yudintsev, M. I. Lapina, S. V. Stefanovsky, S. C. Chae, R. C. Ewing, “Phases formation rate at synthesis of actinide waste forms,” Scientific Basis for Nuclear Waste management XXVI, MRS Symp. Proc., 757, 321-328 (2003).